The Far Infrared Transmission of the Upper Atmosphere

J. A. EDDY, P. J. LÉNA[1] AND R. M. MACQUEEN

High Altitude Observatory, National Center for Atmospheric Research,[2] Boulder, Colo.

(Manuscript received 18 April 1969, in revised form 1 August 1969)

ABSTRACT

Observations of solar and sky radiation in the far infrared (20–125 cm^{-1}) spectral region from a jet aircraft at 12 km altitude are presented, and the presence of absorption lines in the spectra due to H_2O, O_2, O_3 and $(H_2O)_2$ discussed. Estimates of the quantities of precipitable water present above the aircraft are deduced, based upon theoretically generated and instrumentally convolved spectra. An O_3 quantity, based upon observed Q branch absorptions, is given.

The observations are employed to determine 1 cm^{-1} wide regions of low absorption in the 30–125 cm^{-1} spectral range. The fractional transmission of the atmosphere above 12 km altitude in these spectral regions is calculated, based upon recent quantitative laboratory work, considering absorption due to H_2O lines, far wings of H_2O lines, and collision-induced absorption by N_2 and O_2.

1. Introduction

The principal atmospheric absorber in the far infrared (IR) region is water vapor. Due to its effective absorption, ground-based astronomical observations between 15 and 250 cm^{-1} must be made at times of low atmospheric water vapor content from high altitude observing sites. Even under these conditions the atmosphere is essentially opaque to radiation in the 30 to 250 cm^{-1} range; however ground-based observations have indicated the presence of atmospheric "windows" in the 22 and 28 cm^{-1} regions (Gebbie, 1957; Farmer and Key, 1965).

To observe the far IR solar spectrum, one can employ platforms above a substantial fraction of the telluric water vapor. Then regions of absorption due to additional atmospheric constituents may be distinguished. Far IR observations of the sky and extraterrestrial sources have been attempted previously from balloons, aircraft and rockets, and some relevant atmospheric spectra have been published. From balloon observations, the Meudon Infrared Group obtained spectra in the 70 to 160 cm^{-1} region with maximum resolution of 0.25 cm^{-1}, from observing altitudes of 28.4 and 25.0 km. They derived precipitable water quantities of $0.022\pm0.006\ \mu$ and $0.077\pm0.015\ \mu$, respectively, by far the lowest quantities measured in the stratosphere (Gay *et al.*, 1968). Analysis of their non-water vapor lines has not been published. Gebbie and his co-workers obtained spectra of the sky in emission from a high altitude jet aircraft on several occasions, with maximum resolutions $\geqslant 1$ cm^{-1}, over the spectral range 15–65 cm^{-1} (Bader *et al.*, 1967; Gebbie *et al.*, 1968a). In addition to the absorption due to stronger water vapor lines, they identified several regions of absorption due to molecular oxygen and ozone. To our knowledge, no far IR atmospheric spectral information has been obtained with rocketborne systems; such observations typically are made with wide bandpass filters to enhance the low signal to noise ratios (Harwit *et al.*, 1966; Feldman *et al.*, 1968).

In the present paper, we present far IR (20–125 cm^{-1}) atmospheric spectra, utilizing the sun as a source, obtained during flights of a jet aircraft at altitudes slightly above 12 km. On the day on which the data presented herein were obtained, the tropopause (here defined as the lowest level where the temperature lapse rate decreases to 2C km^{-1} or less and does not exceed this value in the next higher 2 km) was in all cases above the flight level. Examination of data from U. S. Weather Bureau balloon soundings made at three stations near the flight path of the aircraft indicate that the tropopause was at altitudes of 14.3, 14.8 and 15.1 km. The spectra were obtained under clear overhead sky conditions, for solar elevation angles $65°\pm2°$, during westward flights over the northwestern United States (latitudes 41–43N, longitudes 98–120W).

Following a brief survey of the experimental techniques, the identification of individual lines in the spectra is discussed. Finally, estimates of the absolute transparency of the atmosphere above 12 km altitude are presented, based upon these observations and other recent laboratory measurements (Burch, 1968). A preliminary identification of many lines was presented earlier (MacQueen *et al.*, 1968); the present work adds to and amends the former.

2. Observations

The experimental results presented herein were obtained during a series of flights of the National Aero-

[1] Present affiliation: Observatoire de Paris, France.

[2] The National Center for Atmospheric Research is sponsored by the National Science Foundation.

nautics and Space Administration Convair 990 jet aircraft on 2, 3, 6 and 7 August 1968, from the Ames Research Center, Moffett Field, Calif. A detailed discussion of the apparatus employed appears elsewhere (Eddy *et al.*, 1969a), as does a determination of the brightness temperature of the solar disk in the spectral region observed (Eddy *et al.*, 1969b). We note briefly that the spectra were obtained employing a scanning Michelson interferometer illuminated with solar rays directed by a gyroscopically stabilized tracking system. All spectra are calibrated in absolute units of flux in that they were obtained by chopping the source against a reference blackbody of controlled temperature. Calibration of the system followed from comparison of the spectrum with that obtained in another mode in which the blackbody was chopped against a liquid nitrogen bath approximating a blackbody. The maximum path difference of the Michelson interferometer in all scans was 19.5 mm, which corresponds to a theoretical resolving power of 0.256 cm^{-1}. The interferometer was advanced in a stepped manner, with path increments of 19.05 μ. The determination of the position of zero path difference of the interferometer arms from the recorded interferogram followed the procedure of the Connes (1966) in which the sine and cosine Fourier transformations were computed for a limited range of real path difference on each side of the principal maximum and then used to determine, and hence approximately correct for, the phase offset. The detector was a liquid-helium-cooled germanium bolometer[3] operated at 2.2K, with noise equivalent power 9×10^{-14} W $Hz^{-\frac{1}{2}}$. The signal-to-noise ratio of the individual spectra exceeds 40:1.

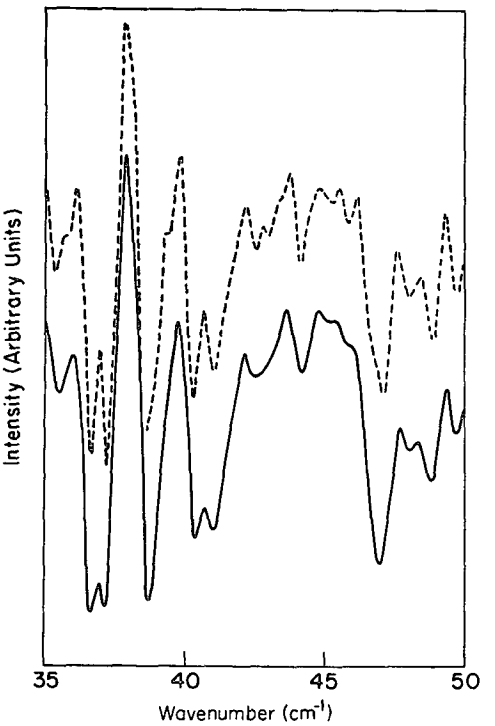

FIG. 1. Comparison of apodized (solid line) and unapodized (broken line) spectra in the spectral range 35–50 cm^{-1}. The sun was the source for the interferogram. The spectra have been displaced vertically to facilitate comparison.

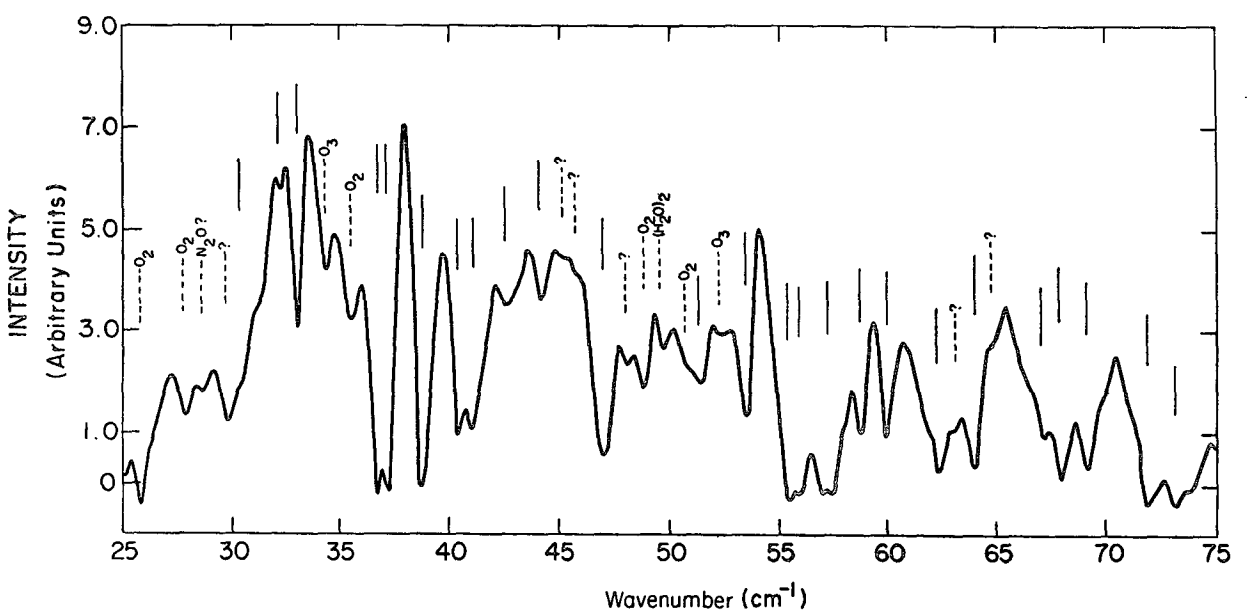

FIG. 2. The 25–75 cm^{-1} spectral region, from a single interferogram. Positions of water vapor absorption are indicated by a solid line, and absorption by other species by dashed lines. No lines only distinguishable on the unapodized spectra are indicated. Note the reduced intensity in the 25–30 cm^{-1} region.

[3] Infrared Laboratories, Tucson, Ariz.

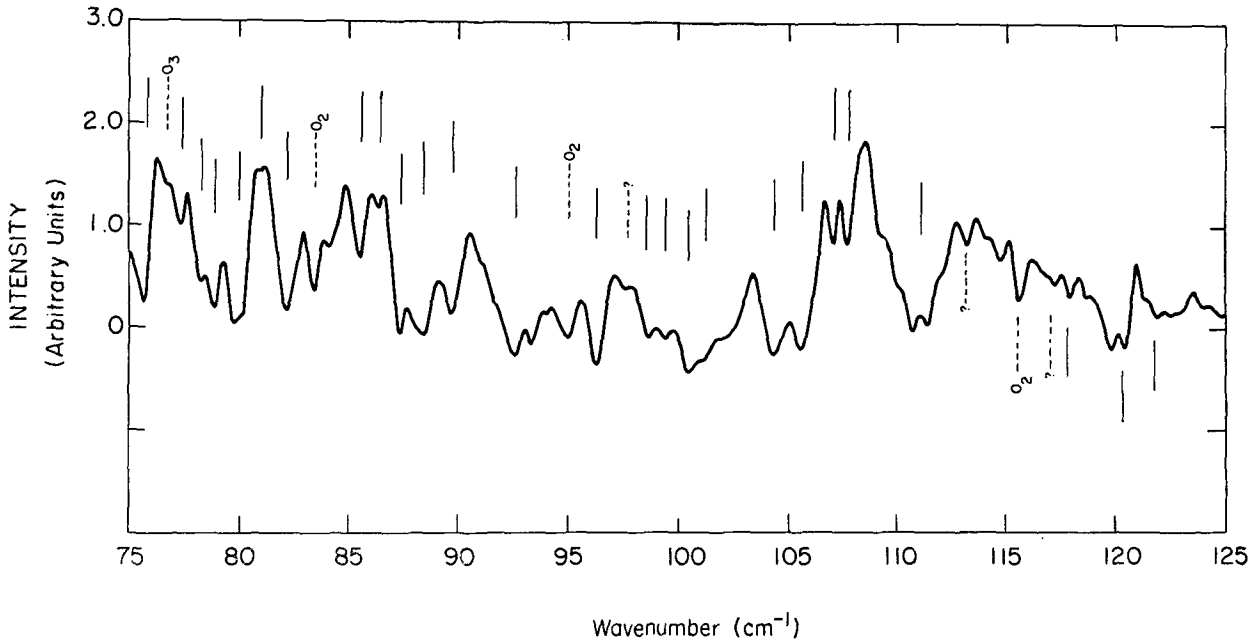

FIG. 3. The 75–125 cm^{-1} region, from the same interferogram as Fig. 2. Negative intensities are the result of chopping the incoming radiation against a 700K reference blackbody.

Due to experimental difficulties concerning electronic vibration and performance of the gyroscopic tracker, the system was not fully optimized until the flight of 7 August, and all data discussed herein are from that flight. During the period aloft nine spectra were obtained employing the nitrogen bath source, thirteen with the sun as the source, and ten of the sky emission. The latter spectra were necessary in eliminating emission from the sky and window for the purpose of the solar temperature determination. The intensity of the solar spectra below 30 cm^{-1} is relatively weak compared to the same spectral region of the sky and calibration spectra (see Section 3e). The origin of this apparent suppression is as yet unexplained; however, the weak signals of the solar spectra make it more advantageous to analyze spectra made in this region using the emission of the sky as the source, even though the signal-to-noise ratio is considerably poorer. These sky spectra were made prior to and following each pair of solar spectra, 10° from the sun in the solar almucantar.

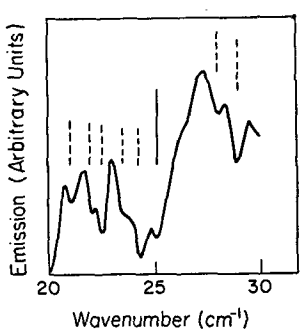

FIG. 4. The 20–30 cm^{-1} region of a single sky interferogram, obtained by admitting the emission from the sky, 10° from the sun, in the solar almucantar. The spectrum has been inverted, i.e., increased sky emission is downward.

Spectra presented herein, with a single exception (Fig. 1), are the result of the Fourier cosine inversion of the interferogram, apodization employing a triangular function, and fifth-order polynomial fitting of the data points. Figures are the result of tracings of the computer output. The effect of such apodization has been well studied; in addition to partially removing the spurious side lobes of the instrumental function, the width of the central maximum is increased somewhat, with a resulting decrease in effective spectral resolution. It is possibly misleading to examine unapodized spectra alone, but in conjunction with the apodized spectra they may provide valuable information concerning barely resolved lines (Connes, P. and J., 1966; Richards, 1967). Such an example appears in Fig. 1, which depicts the 35–50 cm^{-1} region and clearly indicates the usefulness of the comparison.

Figs. 2 and 3 present the results of a single solar scan from the flight of 7 August over the range 25–125 cm^{-1}. The shape of the spectral envelope represents the convolution of instrumental factors (i.e., beam-splitter efficiency, aircraft window transmission, etc.) and the Planck radiation efficiency of the sun, sky, window and reference blackbody emission.

Fig. 4 presents an example of the sky spectra in the range 20–30 cm^{-1}. Discussion of many of the spectral features in Figs. 2–4 will follow in Section 3.

An example illustrating the reproducibility of the observed solar spectra appears in Fig. 5. The three

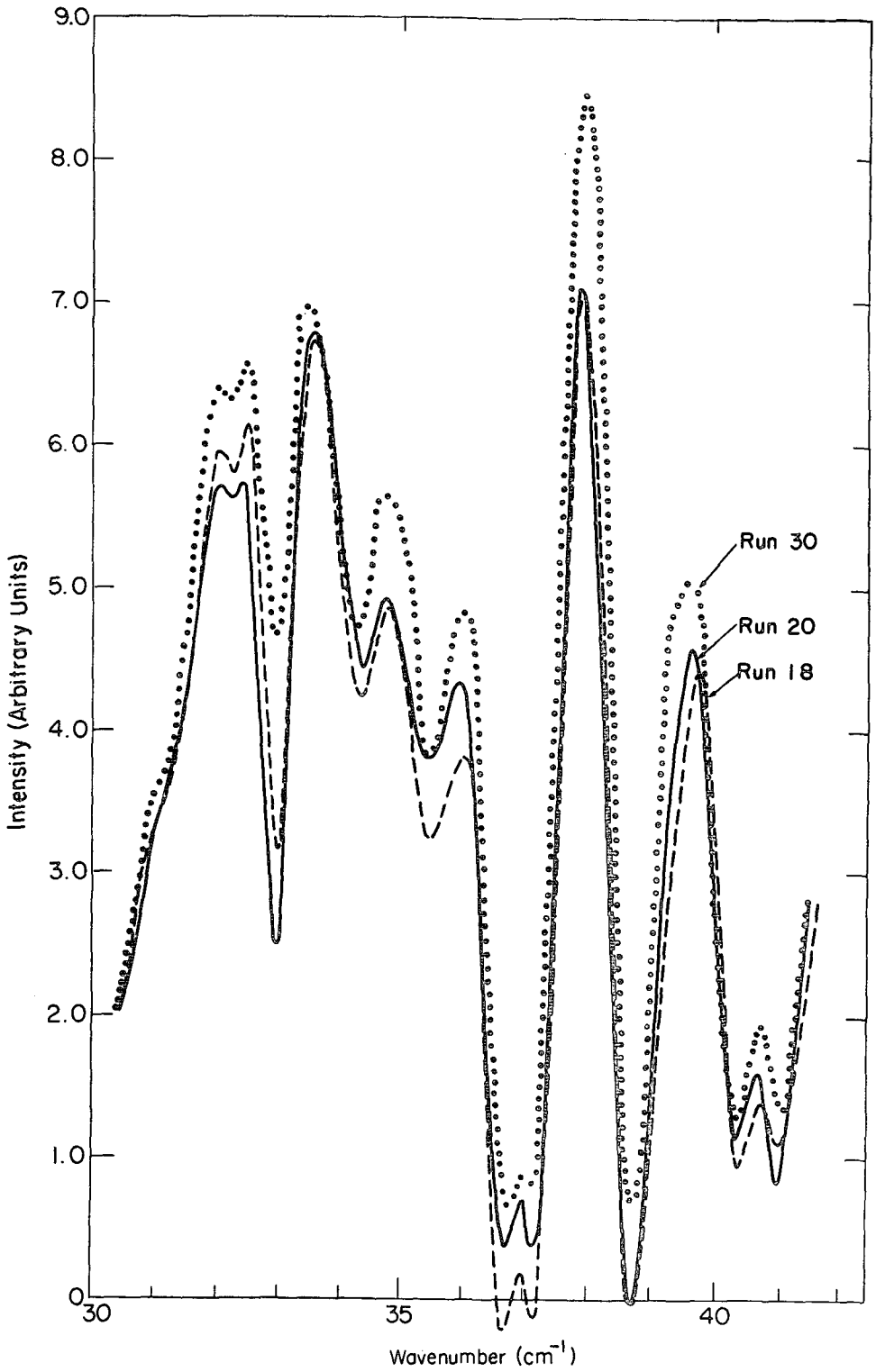

FIG. 5. An example of the reproducibility of the spectral features. The three spectra are from interferograms obtained over a 55-min period, and show the effect of decreasing water vapor quantities through that observing period.

spectra, obtained over a total elapsed time of about 55 min, indicate the excellent repeatability of the various spectral features, and provide some measure of the noise in the spectral range presented. The most favorable range is 30–42 cm^{-1}, combining high atmospheric and window transmissions, and maximum beamsplitter efficiency.

The positions of the spectral features in the following discussion are indicated to the nearest 0.05 cm^{-1}. No correction to the quoted frequencies because of the finite solid angle of acceptance of the interferometer have been applied; the correction is at most (i.e., at the highest frequencies observed) 6.8×10^{-4} cm^{-1}.

It is important to note that the negative values of intensity are not necessarily a measure of the inherent noise in the spectra, or imperfect phase correction, but rather are a result of the chopping mode of the system. When viewing the sun, the net signal received by the detector is the sum of the emission of the sun, sky and window less that of the reference blackbody at a temperature of 700K. In spectral regions where the atmospheric and window transmissions are both low, the algebraic sense of the net signal is negative. This is especially apparent at the high-frequency end of the spectrum, where low window and sky transmissions prevail.

3. Atmospheric constituents

a. Water vapor

The positions, strengths and widths of lines in the far IR due to $H_2{}^{16}O$, $HD^{16}O$ and $H_2{}^{17}O$ have been calculated by Benedict and Kaplan (private communication), with a positional accuracy of at least 0.01 cm^{-1}, and an uncertainty in the strengths of strong lines of about $\pm5\%$. The calculated widths are those due to N_2 broadening (Benedict and Kaplan, 1959). A partial tabulation, including lines in the region 0.74–38.79 cm^{-1}, has appeared recently (Burch, 1968).

The above information has allowed the identification of numerous water vapor lines in the aircraft spectra; these lines are noted with solid lines at the appropriate positions in Figs. 2 and 3. With the resolution employed, it is found that lines whose strength $S\gtrsim60$ cm^{-1} per (gm cm^{-2}) are unambiguously identifiable, provided the lines are in regions of weak or slowly varying absorption (cf. the 30.56 and 32.37 cm^{-1} lines, whose strengths are 59.75 and 56.96, respectively).

Employing the parameters given by Benedict and Kaplan, adopting a line shape and assuming a form for the instrumental function, the quantity of water vapor causing the observed absorption may be estimated, if the levels of zero and 100% transmission are known. Discussion of the choice of the appropriate line shape will be deferred until Section 4a; the Zhevakin-Naumov (1963) shape has been used in these calculations.

For the case of a well-aligned interferometer, employing linear (triangular) apodization, the instrumental function is

$$R=\Delta_{\max}\left\{\frac{\sin\pi(\nu-\nu')\Delta_{\max}}{\pi(\nu-\nu')\Delta_{\max}}\right\}^2, \tag{1}$$

where $\Delta_{\max}$ is the maximum path difference of the interferometer. Specification of the 100% level of the spectra follows *a posteriori* from examination of theoretical water vapor spectra and knowledge of other absorbers in the spectral region in question (see Section 4). An additional complication is that there remained in the instrument inside the aircraft a residual quantity of water vapor, despite continuous N_2 purging and the reduced cabin pressure (7.2×10^{-1} atm). The cabin temperature was about 300K. Analysis of the various scans made while chopping between the reference nitrogen bath and the temperature-controlled blackbody indicate that the total precipitable water content in the instrument was approximately 3.0 μ, an amount consistent with the equilibrium quantity expected in the rather well-controlled environment of the aircraft cabin.

With the above information the precipitable water quantities for the atmosphere have been determined from runs 18, 20 and 30 (Fig. 5) and are 5.5 ± 0.5 μ, 2.75 ± 0.5 μ and 0.5 ± 0.25 μ, respectively. These values are for zenith angle 25°, and are based upon the assumption of an unchanging water content (3 μ) in the instrument. Only weak lines have been employed in the analysis, so that corrections for sky emission are then negligible.

The above values for the amount of precipitable water above the aircraft appear to be consistent with past measurements; for example, an average of the compilation of Junge (1963) and the measurements of Sissenwine *et al.* (1968) yield an approximate average amount of 2.5 μ of precipitable water above 12 km for middle latitudes in summer, but a large variance from the value would not be unexpected. The measurements of Sissenwine *et al.* are especially relevant, since they were made at the approximate latitudes and longitudes of our flight path. The decrease in precipitable water content as the flight progressed was confirmed by a far IR broad spectral bandpass radiation monitor employing a golay cell detector installed so as to view the incoming radiation chopped against the temperature controlled blackbody (see Fig. 6). It is apparent the *sky emission* decreased with time, corresponding to a decrease in water vapor content above the aircraft. The rms noise in the golay signal is on the order of 2%. The elapsed time between runs 18 and 20 was about 7 min and that between runs 20 and 30 ~48 min. Hence, for the approximate aircraft speed of 750 km hr^{-1}, a fractional change for the horizontal distribution of the quantity of water vapor is found to be about

3×10^{-3} km^{-1} for this particular day, at the flight latitudes of 41–43N over the northwestern United States (longitudes 97–120W). This result may be compared with a change of less than 5×10^{-4} km^{-1} found during a flight over the middle Pacific Ocean on 22 October 1967, at an altitude of 12 km between latitudes 10–15N. In the earlier flight, however, the water content was observed to gradually *increase* during the 2-hr period of observations (Eddy and MacQueen, 1969).

b. Oxygen

As noted in Section 1, several regions of absorption in spectra obtained at aircraft altitudes have been attributed to magnetic dipole transitions of the oxygen molecule (Gebbie *et al.*, 1966, 1968a,b). Eight such features have been identified in the new spectra, and are presented in Table 1. The predicted positions have been deduced from the energy levels of the oxygen molecule determined by Babcock and Herzberg (1948), and the microwave splittings observed by Burkhalter *et al.* (1950). The approximate relative intensities shown in Table 1 were derived from the observations for an assumed temperature of 220K, employing the dipole matrix elements of Tinkham and Strandberg (1955). Several of the stronger transitions ($\Delta J=0$) in the spectral region 25–125 cm^{-1} cannot be distinguished from nearby strong water vapor absorption with the resolution employed in the present experiment (cf. the $J=6$, 10, 12, 18 and 20 transitions). No relative intensities have been determined from these spectra for the weaker $\Delta J=1$ transitions. Within the rather large experimental uncertainties, the relative intensities deduced from these measurements agree with the predicted intensities of Tinkham and Strandberg.

c. Ozone

Historically, optical determinations of ozone quantities in the atmosphere have utilized the Hartley, Huggins and Chappuis bands in the near ultraviolet and visible spectral region; the ν_3 fundamental band at

TABLE 1. Observed oxygen transitions (25–125 cm^{-1}).

$\nu_{observed}$	$\nu_{theoretical}$	Transition	Relative intensity Predicted	Observed[b]
25.80[a]	25.81	$K3$–5, $J4$–4	1.3	0.9
27.80[c]	27.82	$K3$–5, $J4$–5	0.4	—
35.40[a]	35.40	$K5$–7, $J5$–6	0.04	—
48.95	48.90	$K7$–9, $J8$–8	1.6	1.6
51.00	50.85	$K7$–9, $J8$–9	0.5	—
83.45[a]	83.48	$K13$–15, $J14$–14	0.8	1.2
95.00[a]	94.96	$K15$–17, $J16$–16	0.6	0.8
115.70[a]	115.73	$K19$–21, $J19$–20	—	—

[a] Lines not previously observed in the atmosphere.
[b] Normalized to the 48.95 cm^{-1} line. The estimated uncertainty is ±20%, but larger for the 25.80 cm^{-1} line where the water overlap correction is large.
[c] Blended with Q4 branch of O_3 (see Table 2).

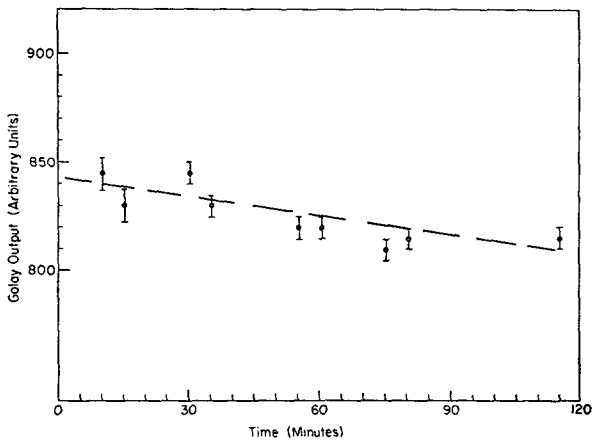

FIG. 6. Sky emission vs time, as recorded by a broad spectral bandpass system.

1043 cm^{-1} has been utilized by Adel (1947) and others to determine ozone emission characteristics. Recent advances in far IR technology have made it possible to estimate the quantity of atmospheric ozone from far IR spectra.

Laboratory far IR data (Gebbie *et al.*, 1960) allowed the tentative identification of ozone as responsible for two features observed in spectra taken from mountaintop; subsequently, aircraft spectra (Gebbie *et al.*, 1968a) confirmed the presence of the Q_2, Q_3 and Q_4 branches of ozone at 16.8, 21.8 and 27.8 cm^{-1}. The present aircraft results overlap and extend the former results (see Table 2).

The positions of the "centers of gravity" of the band heads, summed over the instrumental width, are deduced from the work of Gora (1959). The Q_6, Q_7 and Q_9 branches cannot be separated from neighboring water vapor lines, while identification of the Q_{11} branch at 70.8 cm^{-1} cannot be certain, even with the unapodized spectra. Employing the calculated absorption coefficients at line center and a Lorentz line shape with half-width 0.078 cm^{-1} at 1 atm and 20C (Walshaw, 1955), and making corrections for the overlap of neighboring water vapor lines, an approximate quantity of absorber has been deduced. The Q_3, Q_5 and Q_8 branches have been utilized so as to minimize the latter correction. A

TABLE 2. Observed ozone Q-branches (25–125 cm^{-1}).

$\nu_{observed}$	$\nu_{theoretical}$	Branch
22.00	~21.9	Q_3
27.80	~27.8	Q_4
34.35[a]	~34.3	Q_5
52.75[a]	~52.8	Q_8
65.00[a,b]	~64.9	Q_{10}
76.75[a,b]	~76.8	Q_{12}
82.70[a,b]	~82.6	Q_{13}

[a] Lines not previously observed in the atmosphere.
[b] Identified from unapodized spectra.

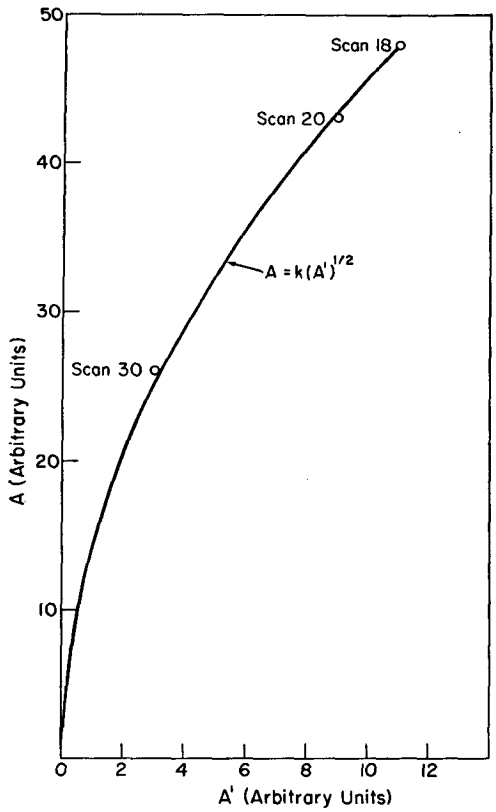

FIG. 7. Water absorption A of the $5_{-2}-4_2$ (32.37 cm^{-1}) monomer vs absorption A' in the 49.70 cm^{-1} region. The square root dependence is consistent with predictions of the behavior of the absorption of the water vapor dimer.

simple average of the results from the three regions yields an ozone quantity above 12 km of $2.5\pm0.6\times10^{-1}$ cm STP, corrected to zenith. Allowing for 8.5% of the total ozone quantity residing below 12 km (cf. Craig, 1965), the total quantity of atmospheric ozone is $2.7\pm0.6\times10^{-1}$ cm STP, to be compared with 3.0×10^{-1} cm (London, 1963) and 2.9×10^{-1} cm (Godson, 1960) for latitude 40N in summer (August). Such agreement is surprising in view of the uncertainties involved in a determination of this type.

d. Water vapor dimer

There is considerable uncertainty as to the role of the water vapor dimer in far IR absorption. Viktorova and Zhevakin (1967a) have calculated the absorption coefficient of the dimer in this region, and have found its continuum absorption to equal or exceed that of the monomer in the spectral range 1–10 cm^{-1} for the conditions $\rho_{H_2O}=7.5$ gm m^{-3}, $p=1$ atm and $T=283$K. Employing a simple linear model of the molecule, the same authors (1967b) found that the positions of the Q branches in the pure rotational spectrum of the dimer (assumed to be a symmetric top) are given by the usual expression

$$\nu=\frac{1}{c}(2K+1), \quad K=0,1,2,\cdots, \tag{2}$$

where c is a constant relating the nodal angles of the centers of mass of the water molecules in the dimer configuration (Burkhard and Irvin, 1955), and K is the quantum number of the component of angular momentum along the internal rotation axis. They interpreted the laboratory observations of an unexplained feature at 49.5 cm^{-1} (Furashov, 1966; Yaroslavskii and Stanevich, 1959) as being due to transitions of the Q branch from levels with $K=3$. Hence, they found $1/c=7.07$ cm^{-1}, as compared with the theoretical value of 6.75 cm^{-1}. To the present authors' knowledge, no additional laboratory observations of the 49.5 cm^{-1} feature have been successful. However, mountaintop and recent laboratory observations have indicated a region of anomalous absorption features in the 7–9 cm^{-1} spectral range, one of which may be due to the dimer Q branch with $K=0$ (Gebbie *et* al., 1968b, 1969). The latter studies recently have verified the predicted dimeric pressure dependence of this absorption (see below).

The present aircraft observations indicate the presence of an absorption feature at 49.70 cm^{-1} (Fig. 2) which is distinct enough to prompt examination of the correlation of the strength of this feature with the water content deduced from the depths of the monomer absorption lines. This correlation is illustrated in Fig. 7, in which the $5_{-2}-4_2$ (32.37 cm^{-1}) monomer absorption A is plotted against the absorption A' due to the feature at 49.70 cm^{-1}. The observed points follow closely a form $A\propto(A')^{\frac{1}{2}}$ in agreement with the predicted behavior of the water vapor dimer (Viktorova, 1964). Two additional features substantiate the conclusion that the 49.70 cm^{-1} feature is due to the dimer Q branch with $K=3$. First, examination of the 35–36 cm^{-1} region of the unapodized spectra (Fig. 1) clearly indicates that the feature at 35.40 cm^{-1} is a blend with an additional feature near 35.6 cm^{-1}. Precise determination of the frequency is not possible, but this feature may be the dimer Q branch for levels $K=2$. Second, the sky spectrum (Fig. 4) shows a feature at 21.20 cm^{-1} which may be attributed to the Q branch for $K=1$. Within the resolution limits of these observations, then, there appears to be confirmation of three spectral features due to dimer Q branch absorption, and the constant $1/c$ is found to be 7.10 ± 0.02 cm^{-1}. The fact, however, that for the observed monomer water vapor quantities, these dimer features are visible, in contrast to theoretical predictions (Viktorova and Zhevakin, 1967a), clearly indicates the need for additional theoretical and experimental studies of the pressure and temperature dependence of the relative concentration and absorptive properties of dimers.

e. Additional species

In the sky and solar spectra additional regions of absorption are present which cannot be attributed to the above molecules. For example, such lines appear in the sky spectra at 22.60, 23.50, 24.30 and 28.65 cm^{-1}, and in the solar spectra at 48.10, 83.45 and 84.20 cm^{-1}. Additionally, examination of the unapodized solar spectra indicates numerous barely resolved regions, some of which may simply be attributed to noise. Such uncertainty precludes any quantitative discussion. A feature at 29.70 cm^{-1} reported earlier (MacQueen *et al.*, 1968) has been found to be inconsistently repeatable, and hence may be of spurious origin.

Absorbers which might possibly give rise to the above seven lines include N_2O, CO, NO and NO_2 as the more likely candidates. However, comparison of laboratory data (Palik and Rao, 1956; Bird *et al.*, 1958) and calculated spectra (Bird, 1956) with the observed lines leads to ambiguous results. There is good correlation, for example, within experimental uncertainty, between the features observed at 22.65, 23.50, 24.30 and 28.65 cm^{-1} with the positions of the pure rotational lines of N_2O corresponding to $J=26$, 27, 28 and 33, respectively, where J is the rotational quantum number of the lower level of the transition. However, since under stratospheric conditions one would expect the level $J\sim18$ to have maximum population, the lines at 20.90 and 21.77 cm^{-1}, corresponding to $J=23$ and 24, should be prominent. Their apparent absence from the observed spectra therefore casts doubt upon the other identifications. In addition, if the quantity of N_2O present in the upper atmosphere is assumed to be that determined by Seeley and Houghton (1961), then the calculated absorption in the individual rotational lines is only a small fraction of that observed in the above lines. Agreement is found between the $J+\frac{1}{2}=6$, $^2\pi_{\frac{3}{2}}$ line of NO (22.37 cm^{-1}) and the observed 22.60 cm^{-1} line, but the companion $^2\pi_{\frac{1}{2}}$ line at 21.71 cm^{-1} is absent (Palik and Rao, 1956). No agreement between lines of CO and NO_2 and the observed lines occurs.

Of interest is the recent report (Gebbie *et al.*, 1968b) of an apparent suppression in the 23 cm^{-1} region, and an observed asymmetry in the low frequency side of the $2_{-2}-2_0$ water vapor transition at 25.08 cm^{-1}, in solar spectra obtained at mountaintop. Fig. 4 indicates our sky spectra for the region in question, and shows that the asymmetry evidently arises from the unknown absorptions at 23.50 and 24.30 cm^{-1}. Concerning the former anomaly, we find substantially no difference between the ratio of the intensities observed at 28 and 23 cm^{-1} in our interior calibration runs, and the ratio obtained from the sky emission spectra. The average ratio from the calibration runs is 1.82 ± 0.20 and that from the sky emission runs is 1.91 ± 0.15. It therefore appears that the origin of the suppression observed at mountaintop at 23 cm^{-1} is either solar, lower atmospheric (<12 km), or instrumental. Further discussion of the origin of the suppression appears in Eddy *et al.* (1969b).

4. Transparency of the atmosphere above 12 km

With a knowledge of the positions and approximate strengths of the various molecular lines in the far IR, it is possible to calculate the transmission of the atmosphere above 12 km, for the case of instrumentally convolved lines.

The total absorption in the far IR spectral region arises from 1) line absorption due to discrete transitions of the various molecular species present, and continuum absorption, which includes both 2) that due to the far wings of molecular lines, and 3) induced effects.

Determination of 1) in the case of water vapor was made using the data of Benedict and Kaplan (1959, 1964), and specifying an appropriate line shape, indicated by recent laboratory absorption studies. The present study has also indicated the spectral regions where additional molecular species absorb, and these regions have been avoided so as to reduce the number of uncertainties in the calculation.

Recent laboratory measurements also permit estimates of 2) for the case of water vapor. Attenuation due to induced absorption of N_2 and O_2 can be estimated from laboratory measurements of the absorption coefficient, if assumptions about the pressure and temperature of the atmosphere at the level in question are made.

Disagreement between calculated and observed transmissions in the far IR has characterized the literature over the past decade (Bastin, 1966; Hall, 1967); only some of the discrepancies have been attributable to the large corrections required to eliminate the broad instrument functions involved in the measurements. Until the recent work of Burch (1968), no reliable quantitative measures of laboratory transmission in the far IR were available. In addition, calculated far IR transmissions, convolved with instrumental functions, are scarce. Turon-Lacarrieu and Verdet (1968) have recently published transmission curves for balloon altitudes (30 km), including the effects of an instrumental function 0.5 cm^{-1} broad; they also present unconvolved transmission curves for various quantities of precipitable water ranging from 0.075 to 75 μ.

The experimental and theoretical bases for the specification of the various parameters required for the determination of the total transmission in the far IR are discussed below. The fractional transmissions (averaged over 1 cm^{-1} intervals) which result when the three sources of opacity are considered are given in Table 3 for several water vapor amounts. To reiterate, these spectral intervals were chosen so as to avoid line absorption by molecules other than water.

a. Water vapor line absorption

The measurements of Burch have shown that the Lorentz and Zhevakin-Naumov line shapes are essentially equivalent at frequencies higher than 20 cm^{-1}; both, however, overestimated the observed absorption at lower frequencies, the Lorentz shape being more in error. The Zhevakin-Naumov absorption coefficient has been employed in the present work; that is,

$$K(\nu)=\frac{S\,4\nu\nu_0\alpha}{\pi[(\nu^2-\nu_0^2)^2+4\nu^2\alpha^2]}, \tag{3}$$

with α the half-width, S the line strength, and ν_0 the frequency of line center. In calculating the transmissions, the data of Benedict and Kaplan for α, S and ν_0 have been used. Their data refer to nitrogen-broadened lines only; to account for the effects of broadening by oxygen in air, values for the widths have been multiplied by 0.90 (Benedict and Kaplan, 1964; Rusk, 1965). The line *shape* has been assumed to remain the same. Due to the relative partial pressures of N_2 and H_2O in the upper atmosphere, the effects of self-broadening due to H_2O–H_2O collisions can be neglected.

A theoretical spectrum of water vapor, including the 103 lines between 20–125 cm^{-1} whose strength $S \geq 10$ cm^{-1} per (gm cm^{-2}) (for $T=220$K), has been generated and convolved with the theoretical instrumental function of Eq. (1). The pressure has been assumed to be 2×10^{-1} atm, corresponding to an altitude of approximately 12 km. Spectra were calculated for water quantities ranging from 2–20 precipitable microns. (A spectrum, corresponding to the physical conditions present inside the aircraft was calculated also, and the resultant product of transmissions used to determine the water quantities in the atmosphere as shown in Section 3a.) Because the water vapor content in the atmosphere is concentrated toward lower altitudes, use of the pressure at the altitude of observation is more appropriate in a simple model than use of an average above the observation level. The transmission in "window" regions calculated employing this assumption is approximately 1% lower than that determined using the Curtis-Godson approximation over the 12–15 km altitude range.

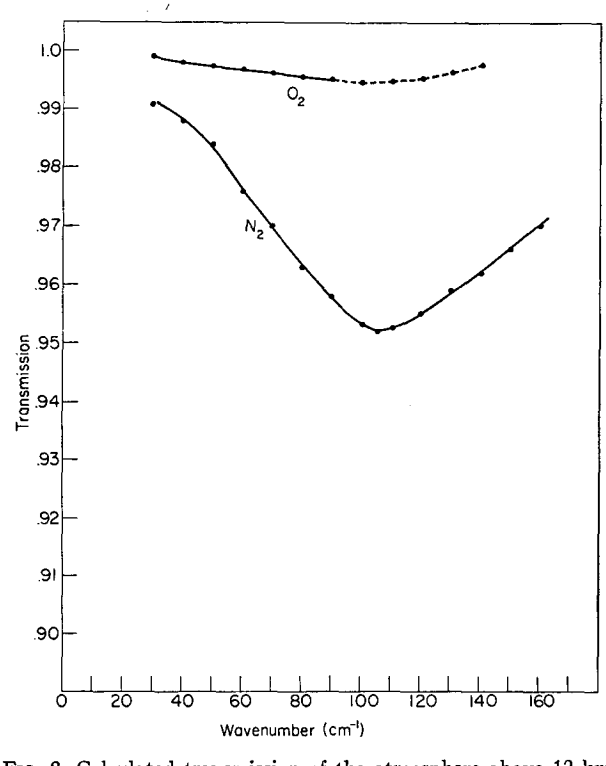

FIG. 8. Calculated transmission of the atmosphere above 12 km altitude for the case of collision-induced absorption of N_2 and O_2.

b. Continuum absorption—far wings of water vapor

The actual transmission at frequencies between various discrete lines in the water vapor spectrum is not accurately represented by any line absorption coefficient. Burch (1968), using controlled pressures and water quantities in the laboratory, has determined a continuum absorption coefficient in the spectral region 12.7–36.0 cm^{-1} from the difference between a calculated transmission, assuming the Van Vleck-Weisskopf line shape, and the observed transmission. His results also permit a continuous absorption coefficient to be determined when the Zhevakin-Naumov line shape is employed in calculating transmission.

The continuum absorption coefficient should be proportional to pressure since its origin is the far wings of lines; the temperature dependence is less certain, and is here assumed as a first approximation to be the same as the temperature dependence of the individual lines.

Burch's results show that at frequencies higher than 30 cm^{-1}, the continuum coefficient is approximately 10% of that predicted for the wings by the line absorption coefficient itself. This relative magnitude has been assumed to hold between water lines up to 125 cm^{-1}.

c. Induced continuum absorption

An additional source of continuum absorption is that due to collisionally induced dipole moments of atmospheric gases, principally nitrogen and oxygen. Laboratory measurements indicate that the variation of the induced absorption coefficient with frequency approximately follows a bell-shaped curve, peaked at 105 cm^{-1} in the case of nitrogen (Heastie and Martin, 1962; Gebbie *et al.*, 1963; Bosomworth and Gush, 1965). Because the absorption coefficient for such a process is proportional both to the number of gas molecules and to the rate of collisions, it is ultimately a function of the square of the pressure. To determine the transmission, the attenuation of radiation is written as

$$dI/I=-\beta[p(h)]^2dh, \tag{4}$$

TABLE 3. Calculated total transmission (30–145 cm^{-1}).

ν (cm^{-1})	Precipitable water content (μ) 20	10	6	2
31.5[a]	0.96	0.96	0.98	0.98
43.0	0.91	0.96	0.96	0.98
45.0	0.94	0.96	0.97	0.98
50.0	0.96	0.97	0.97	0.98
60.8	0.81	0.88	0.91	0.94
66.0	0.92	0.95	0.95	0.96
70.2	0.80	0.88	0.91	0.95
77.0	0.70	0.82	0.87	0.92
84.1	0.82	0.88	0.92	0.94
90.5	0.55	0.72	0.80	0.90
95.0	0.69	0.80	0.85	0.92
103.0	0.64	0.77	0.81	0.90
109.0	0.79	0.87	0.90	0.93
115.0	0.91	0.93	0.94	0.95
124.0	0.61	0.73	0.80	0.89
129.5	0.69	0.80	0.85	0.91
134.7	0.64	0.78	0.84	0.92
136.7	0.74	0.85	0.90	0.94
144.0	0.91	0.93	0.94	0.96

[a] Transmissions are averaged over 1 cm^{-1} band centered on the given frequency.

where β is the absorption coefficient (cm^{-1} atm^{-2}) and $p(h)$ the pressure dependence on height h. Assuming an exponential decrease in pressure above reference height h_1, and a constant scale height H for the species (N_2 or O_2), the transmission becomes

$$T=\exp\left[-\beta(\nu)p^2(h_1)\frac{H}{2}\right]. \quad (5)$$

The respective scale heights for N_2 and O_2 are about 6.8 and 6.0 km, when $T=220$K. Transmissions calculated from (5), employing the measured values of the absorption coefficient β for N_2 and O_2, are plotted in Fig. 8. Values of β for O_2 in the region above 90 cm^{-1} have not been measured, and the O_2 curve has been extrapolated assuming the same relative magnitude and shape as the N_2 curve. It is to be noted that pressure-induced effects alone can account for 5% absorption near 100 cm^{-1}.

The results of the calculations are summarized in Table 3. The total transmission, averaged over 1 cm^{-1} intervals is presented, representing the product of the transmission due to the line absorption coefficient, that due to an assumed continuum coefficient of the far wings of water vapor lines, and that due to the collision-induced phenomena of N_2 and O_2. The spectral regions have been chosen to fall between water vapor lines, and to exlude the line absorptions of other molecules, based upon the results of Section 3. Total transmission values are given for precipitable water quantities of 20, 10, 6 and 2μ, to cover a broad range of conditions. Table 3 indicates that there are numerous spectral regions of 1 cm^{-1} width in which the transmission exceeds 70%, even for relatively large amounts of upper atmospheric water vapor. Further, these results demonstrate the feasibility of moderately high resolution far IR spectral measurements of extraterrestrial sources from aircraft altitudes.

Acknowledgments. The authors wish to thank Dr. W. S. Benedict for making available the water vapor absorption data, and R. H. Lee for his invaluable aid in obtaining the observations. We are also indebted to R. V. Helgason and Mrs. Rebecca Marshall for assistance in the computer data analysis. We thank N. Medrud for obtaining and interpreting the Weather Bureau balloonsonde observations, and Dr. J. London for useful comments concerning the manuscript. Finally, we thank the personnel of the Airborne Science Office, NASA Ames Research Center, for their assistance and flight support.

REFERENCES

Adel, A., 1947: Atmospheric temperatures from infrared emission spectra of the moon and earth I. The ozone layer. *Astrophys. J.*, **105**, 406–407.

Babcock, H. D., and L. Herzberg, 1948: Fine structure of the red system of atmospheric oxygen bands. *Astrophys. J.*, **108**, 167–190.

Bader, M., R. Cameron, W. Burroughs and H. Gebbie, 1967: Submillimetre wave observations at an altitude of 40,000 ft. *Nature*, **214**, 377.

Bastin, J. A., 1966: Extreme infrared atmospheric absorption. *Infrared Phys.*, **6**, 209–221.

Benedict, W. S., and L. D. Kaplan, 1959: Calculation of line width in H_2O-N_2 collisions. *J. Chem. Phys.*, **30**, 388–399.

——, and ——, 1964: Calculation of line widths in H_2O-H_2O and H_2O-O_2 collisions. *J. Quant. Spectry. Radiative Transfer*, **4**, 453–469.

Bird, G. R., 1956: Microwave spectrum of NO_2: A rigid rotor analysis. *J. Chem. Phys.*, **25**, 1040–1045.

——, A. Danti and R. C. Lord, 1958: Pure rotational absorption of NO_2 in the 50–200 μ region. *Spectrochim. Acta.*, **12**, 247–252.

Bosomworth, D. R., and H. P. Gush, 1965: Far infrared spectroscopy of compressed gases using a Michelson interferometer. *Japanese J. Appl. Phys.*, **4**, Supplement I, 588–593.

Burch, D. E., 1968: Absorption of infrared radiant energy by CO_2 and H_2O. III. Absorption by H_2O between 0.5 and 36 cm^{-1}. *J. Opt. Soc. Amer.*, **58**, 1383–1394.

Burkhard, D. G., and J. C. Irvin, 1955: Solution of the wave equation for internal rotation of two completely asymmetric molecules. *J. Chem. Phys.*, **23**, 1405–1414.

Burkhalter, J. H., R. S. Anderson, W. V. Smith and W. Gordy, 1950: The fine structure of the microwave absorption spectrum of oxygen. *Phys. Rev.*, **79**, 651–655.

Connes, P., and J. Connes, 1966: Near-infrared planetary spectra by Fourier spectroscopy I. Instruments and results. *J. Opt. Soc. Amer.*, **56**, 896–910.

Craig, R. A., 1965: *The Upper Atmosphere.* New York, Academic Press, 186 pp.

Eddy, J., P. Léna and R. MacQueen, 1969a: *Appl. Opt.* (in press).

——, —— and ——, 1969b: *Solar Physics* (in press).

——, and R. MacQueen, 1969: Infrared scattering observations in the upper atmosphere. *J. Geophys. Res.*, **74**, 3322–3330.

Farmer, C. B., and P. J. Key, 1965: A study of the solar spectrum from 7 μ to 400 μ. *Appl. Opt.*, **4**, 1051–1068.

Feldman, P. D., D. P. McNutt and K. Shivanandan, 1968: Rocket observations of bright celestial infrared sources in Ursa Major. *Astrophys. J. (Letters)*, **154**, 131–136.

Furashov, N. J., 1966: Far infrared absorption by atmospheric water vapor. *Opt. Spectry.*, **20**, 427–435.

Gay, J., J. Lequeux, J. P. Verdet, P. Turon-Lacarrieu, M. Bardet,

J. Roucher and Y. Zeau, 1968: Balloon observations of the far infrared spectrum and brightness temperature of the sun. *Astrophys. Letters*, **2**, 169–172.

Gebbie, H. A., 1957: Detection of submillimeter solar radiation. *Phys. Rev.*, **107**, 1194–1195.

——, N. Stone and C. Walshaw, 1960: Pure rotational association of ozone in the region 125–500 microns. *Nature*, **187**, 765–767.

——, —— and D. Williams, 1963: An interferometric study of the far infrared spectrum of compressed nitrogen. *Mol. Phys.*, **6**, 215–217.

——, W. J. Burroughs, J. A. Robb and G. R. Bird, 1966: Observations of the magnetic dipole rotation spectrum of oxygen. *Nature*, **212**, 66–67.

——, ——, J. E. Harries and R. M. Cameron, 1968a: Submillimeter wave spectroscopy of the earth's atmosphere above 39,000 feet. *Astrophys. J.*, **154**, 405–408.

——, J. Chamberlain and W. J. Burroughs, 1968b: Submillimetre wave solar observations. *Nature*, **220**, 893–895.

——, ——, J. Chamberlain, J. E. Harries, and R. G. Jones, 1969: Dimers of the water molecule in the earth's atmosphere. *Nature*, **221**, 143–145.

Godson, W. L., 1960: Total ozone and the middle stratosphere over arctic and sub-arctic areas in winter and spring. *Quart. J. Roy. Meteor. Soc.*, **86**, 301–317.

Gora, E. K., 1959: The rotational spectrum of ozone. *J. Mol. Spectry.*, **3**, 78–99.

Hall, J. T., 1967: Attenuation of millimeter wavelength radiation by gaseous water. *Appl. Opt.*, **6**, 1391–1398.

Harwit, M., D. P. McNutt, K. Shivanandan and B. J. Zajac, 1966: Results of the first infrared astronomical rocket flight. *Astron. J.*, **71**, 1026–1029.

Heastie, R., and D. H. Martin, 1962: Collision induced absorption of submillimeter radiation by non-polar gases. *Can. J. Phys.*, **40**, 122–127.

Junge, C. E., 1963: *Air Chemistry and Radioactivity*. New York, Academic Press, 4–12.

London, J., 1963: The distribution of total ozone in the Northern Hemisphere. *Beitr. Phys. Atmos.*, **36**, 254–263.

MacQueen, R., J. Eddy and P. Léna, 1968: New far infrared observations of atmospheric molecular lines. *Nature*, **220**, 1112–1113.

Palik, E. D., and K. N. Rao, 1956: Pure rotational spectra of CO, NO and N_2O between 100 and 600μ. *J. Chem. Phys.*, **25**, 1174–1176.

Richards, P. J., 1967: Fourier transform spectroscopy. *Spectroscopic Techniques*, Amsterdam, North-Holland Publ. Co., 33–66.

Rusk, J. R., 1965: Line-breadth study of the 1.64-mm absorption in water vapor. *J. Chem. Phys.*, **42**, 493–500.

Seeley, J. S., and J. T. Houghton, 1961: Spectroscopic observations of the vertical distribution of some minor constituents of the atmosphere. *Infrared Phys.*, **1**, 116–132.

Sissenwine, N., D. Grantham, D. and H. Salmela, 1968: Mid-latitude humidity to 32 km. *J. Atmos. Sci.*, **25**, 1129–1140.

Tinkham, M., and M. W. P. Strandberg, 1955: Thoery of the fine structure of the molecular oxygen ground state. *Phys. Rev.*, **97**, 937–951.

Turon-Lacarrieu, P., and J.-P. Verdet, 1968: Atmospheric absorption from 50 μ to 1 mm. *Ann. Astrophys.*, **31**, 237–243.

Viktorova, A. A., 1964: Concerning the rotational spectrum and the intensity of absorption of water vapor dimers in the atmosphere II. Concentration of dimers. *Radiofizika*, **7**, 424–431.

——, and S. A. Zhevakin, 1967a: Absorption of microwaves in air by water vapor dimers. *Soviet Physics—Dokl.*, **11**, 1065–1068.

——, and ——, 1967b: The water vapor dimer and its spectrum. *Soviet Physics—Dokl.*, **11**, 1059–1062.

Walshaw, C. D., 1955: Line widths in the 9.6 μ band of ozone. *Proc. Phys. Soc., London*, **A68**, 530–534.

Yaroslavskii, N. G., and A. E. Stanevich, 1959: The long wavelength infrared spectrum of H_2O vapor and the absorption spectrum of atmospheric air in the region 20–2500 μ. *Izv. Vysshikh Uchebn Zavedenii Radiofiz.*, **7**, 380–382.

Zhevakin, S. A., and A. P. Naumov, 1963: On the absorption coefficient of electromagnetic waves by water vapors in 10–2 cm band. *Izv. Vysshikh Uchebn Zavedenii Radiofiz.*, **6**, 674–695.